Theor Chem Acc (2016) 135:171
DOI 10.1007/s00214-016-1916-7

REGULAR ARTICLE

Band gap and oxygen vacancy diffusion of anatase (101) surface: the effect of strain

Yayun Zhang[1] · Feng Hao[2] · Chao Liu[1] · Xi Chen[2]

Received: 17 March 2016 / Accepted: 24 May 2016 / Published online: 30 June 2016

Abstract The effects of strain on the band gap and oxygen vacancy diffusion are investigated for the anatase (101) surface through density functional theory calculations. The results show that biaxial strain can effectively shift the band edge of the surface; for example, tensile strain gently reduces the band gap. With respect to the subsurface-to-surface diffusion of oxygen vacancy, energy barrier has a significant dependence on strain. As strain increases, it facilitates O-vacancy diffusion at the clean surface but hinders this migration for the reduced surface in the presence of water. Analysis based on the water adsorption energy indicates that the interplay between O-vacancy and water is weakened with increasing strain.

Keywords Band gap · Oxygen vacancy diffusion · Anatase surface · Strain · Water

1 Introduction

Titanium dioxide (TiO_2) is of great concern for environmental and energy issues recently, since it has extensively potential applications, including anode materials of lithium-ion batteries [1], the redox transformation of organic compounds in wastewater treatments [2], and hydrogen production through water splitting [3]. Among its polymorphs, anatase has attracted increasing interests. However, owing to its intrinsic band structure, the fascinating photocatalytic process is required to be under UV irradiation. Thus, doping TiO_2, including anions or cations, and coupling TiO_2 with narrow band gap semiconductors are the two typical approaches [4, 5], in the spirit of increasing the visible light activity to improve the photocatalytic efficiency, but suffer the fast recombination of the photogenerated electron and hole. As a novel high-performance photocatalyst, TiO_2–graphene exhibits enhanced photocatalytic activity and stability for the degradation of pollutants and highly efficient H_2 evolution [6, 7].

In general, anatase is nanostructured material, offering a large surface area. Growing efforts are therefore directed toward the study of surface [8]. Naturally, anatase TiO_2 crystals are dominated by the (101) facets due to the minimization of surface energy and can be synthesized with a high percentage of (001) facets using hydrofluoric acid as a morphology-controlling agent, inspired by first-principles calculations [9]. More recently, Yu et al. [10] reported an enhanced photocatalytic CO_2-reduction activity over anatase TiO2 with coexposed (001) and (101) facets, attributed to the surface heterojunction.

Apart from experimental investigations, there exist tremendous theoretical studies of the anatase surface with respect to its fundamental physical and chemical properties [11], including surface structure [12–14], electronic structure [15–17], and molecular adsorption [18–24]. At the nanoscale, strain arises inevitably for anatase crystals due to so high surface-to-volume ratios and the interaction with their surroundings. Recently, Darkins et al. [25] found that surface reconstruction leads to the large deformations and stresses for anatase nanoparticles ranging from 2 to 6 nm,

✉ Chao Liu
liuchao@cqu.edu.cn

✉ Xi Chen
xichen@columbia.edu

[1] Key Laboratory of Low-Grade Energy Utilization Technologies and Systems, Ministry of Education, College of Power Engineering, Chongqing University, Chongqing 400030, China

[2] Department of Earth and Environmental Engineering, Columbia Nanomechanics Research Center, Columbia University, New York, NY 10027, USA

confirming that surface strain is inevitable at nanoscale. Accordingly, we here focus on the effect of elastic strain, originating from either surface tension of itself or strain engineering, on the band gap and oxygen vacancy diffusion of the anatase TiO_2 (101) surface.

In previous papers, it is demonstrated that the band structure can be effectively tailored by applying the biaxial strain or uniaxial pressure for anatase bulk [26, 27], and its influence on the band gap of the predominated surface of anatase also needs to be clarified. For the oxygen vacancy, it plays an important role in the surface chemistry of the reduced anatase, especially surface adsorption. For example, water can strongly bind on the (101) surface and then easily dissociate in the vicinity of the subsurface oxygen vacancy [28]. On the other hand, surface oxygen vacancy induces the transformation of peroxo (O_2^{2-}) from the adsorbed O_2 molecule [29] and the dissociation of water through a barrierless pathway [30]. Interestingly, the two reduced TiO_2 surfaces can be related by oxygen vacancy migration from the subsurface to the surface. In this work, by means of energy barrier, the effect of strain on the O-vacancy diffusion kinetics is investigated through first-principles calculations for the TiO_2 (101) surface with and without water adsorption, which contributes to interpreting the role of strain in the surface reactivity.

2 Methods

In our studies, all the calculations are performed using spin-polarized density functional theory (DFT) with the projector augmented wave (PAW) method [31]. The exchange correlation energy of interacting electrons is expressed by using the generalized gradient approximation (GGA) with the Perdew–Burke–Ernzerhof (PBE) functional [32]. The Gaussian smearing method, with the width of the smearing of 0.05, is employed to describe the total energy. It is sufficient for the kinetic energy cutoff of 28 Ry for the plane wave expansion, which ensures that the total energy is converged. The Monkhorst–Pack method, with the Γ-centered k-point grid of $2 \times 3 \times 1$, is adopted for integration in the Brillouin zone. For structural optimizations, the atoms are allowed to relax until the forces on all atoms are converged below the limit of 1×10^{-3} a.u. (~0.05 eV/Å).

Figure 1 shows the configuration of anatase (101) surface. The periodically repeated slab consists of three TiO_2 layers with the in-plane lattice constants 10.44 and 7.61 Å, which correspond to the [010] and [$\bar{1}$01] directions, respectively. A vacuum layer of 15 Å is considered to eliminate the coupling effect of neighboring slabs along the [101] direction. To study the effect of elastic strain on the band gap and diffusion, the principal stretches are applied along epitaxial directions of [010] and [$\bar{1}$01] by changing the sizes of the supercell, and then the lattice parameters are fixed, but all the atoms are allowed to relax. Specially, the highlighted yellow V_O is considered to be a stable defect site for the reduced anatase surface [28], and this subsurface oxygen vacancy is taken to evaluate the influence of strain on oxygen vacancy diffusion to the surface with frozen atoms in the bottom layer. For O-vacancy migration from the subsurface to the surface, the involved atoms are denoted as Ti_{5c}, O_{3c}, and O_{2c} in Fig. 1. To obtain actual diffusion pathways and the corresponding energy barriers, we carry out the climbing image nudged elastic band (CI-NEB) calculations [33], implemented in the Quantum ESPRESSO package [34].

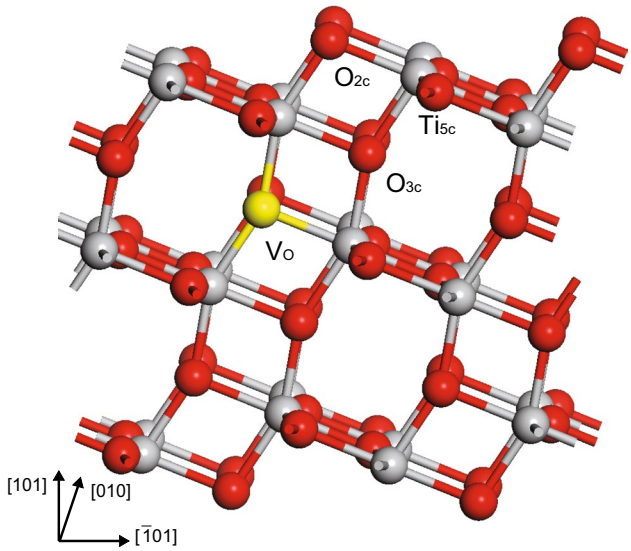

Fig. 1 The structure of anatase TiO_2 (101) surface, where *light gray* represents Ti and *red* is O. It shows the twofold coordinated oxygen O_{2c}, threefold coordinated oxygen O_{3c}, and fivefold coordinated titanium Ti_{5c}, and the subsurface O-vacancy site is highlighted in *yellow*

It is well known that GGA underestimates the band gap, but it is considered to be qualitatively accurate. For other sophisticated methods, such as GW and HSE06, they are very time-consuming despite providing a more precise description of the band structure [35]. In view of our resources, GGA is employed here to calculate the band gap.

3 Results and discussion

To begin with, we obtain density of state (DOS) with regard to anatase TiO_2 bulk to ensure the validity of our calculations. As shown in Fig. 2a, the indirect band gap reads 2.10 eV, which is consistent with the reported result of 2.12 eV, by using GGA-PBE of the same DFT implementation [36].

Figure 2b illustrates the effect of strain on the band gap difference of anatase TiO_2(101) surface in the reference of

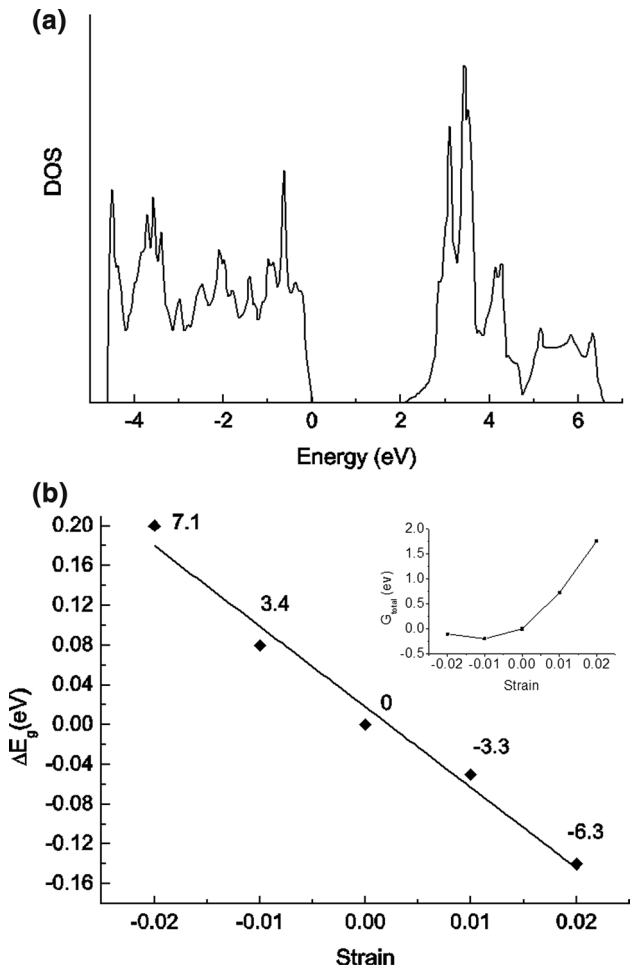

Fig. 2 **a** Density of state for anatase bulk and **b** the strain-dependent band gap and total Gibbs free energy (*insert*) difference of anatase (101) surface with denoted stress difference

that without strain, along with the averaged biaxial stress in the directions of [010] and [$\bar{1}$01]. It can be seen that the band gap is significantly lowered with increasing strain. For example, E_g increases by 200 meV when it experiences a compressive elastic strain of 2 %. It is also interesting to note the total Gibbs free energy change along the stress differences, which is shown in the insert of Fig. 2b. A slight energy change occurs when the surface is compressed. On the contrary, giving a tensile strain increases the total energy dramatically within the range of strain studied. The results of energy change reveal that the anatase TiO_2 surface is tolerable to small compress strain, but the conformation change cannot be neglected when large tensile strain is applied due to the large total Gibbs free energy induced, which are in accordance with previous relevant studies [37–39].

By linear fitting of Fig. 2b, the band gap difference can be represented by lattice strain as $\Delta E_g = 0.018 - 8.1\varepsilon$ eV. It should be noted that usually the GGA substantially predicts a lower band gap, but here the band gap differences are adopted rather than the band gap itself, providing a possibility that enhances the accuracy of the response of the band gap to the applied strain. Simpson et al. [40] reported that a relative misfit strain of 1.3 % was produced for anatase TiO_2 film grown on $SrLaGaO_4$ substrate over that grown on $LaAlO_3$ substrate, leading to a 100 meV redshift in the band gap. As studied here, multiplying the slope of 8.1 eV by the lattice strain gives 105 meV, which agrees with experimental result very well. In addition, it is mentioned above that applying stress can effectively modify the band structure of anatase bulk, and the slopes for *ab*-plane are 43.5 and 35.3 meV/GPa reported by Thulin et al. [26] and Yin et al. [27], respectively. Using the calculated stresses in Fig. 2b, it yields 24.2 meV/GPa for the surface. This relative low slope originates from *c*-axis included in the epitaxial direction for the (101) surface, namely [$\bar{1}$01]. It has been demonstrated that stress in *c*-axis has an opposite impact on tuning the band gap compared to that of *ab*-plane [27]; as a result, the effect of biaxial strain on band gap of (101) surface is partially offset. Therefore, it is reasonable to use the equation obtained in present work to describe the relationship between the band gap difference and lattice strain in the anatase TiO_2(101) surface.

Next, in terms of energy barrier, oxygen vacancy diffusion at the (101) surface is investigated under varying in-plane strain. Neglecting the dependence on the oxygen chemical potential, we can simplify the formation energy of oxygen vacancy E_{form} as [41].

$$E_{form} = E_{tot} - E_{def} + \frac{1}{2}E(O_2) \quad (1)$$

where E_{tot} is the total energy of pristine anatase TiO_2(101) surface, E_{def} is the energy of its off-stoichiometric counterpart with the subsurface O-vacancy, and $E(O_2)$ is the total energy of an O_2 molecule. Cheng and Selloni [41] compared the formation energies for different inequivalent surface and subsurface O-vacancy defects and found V_O, depicted in Fig. 1, is the energetically most favorable defect with the energy of 4.03 eV for the slab containing 108 atoms. The V_O formation energy calculated is 4.11 eV, slightly higher than the above reported value due to a smaller system of 72 atoms employed here which limits the sufficient relaxation around the O-vacancy.

As a center of trapping excess electrons, oxygen vacancy is a critical factor to enhance chemical reactivity for the TiO_2(101) surface [42]. However, owing to the lower formation energy, O-vacancy trends to reside the subsurface or deeper inside the bulk and could not spontaneously migrate to the clean surface. More recently, it is found both theoretically and experimentally that O_2 molecule adsorbed on the (101) surface of anatase greatly facilitates oxygen vacancy diffusing from the subsurface to surface [29]. Additionally,

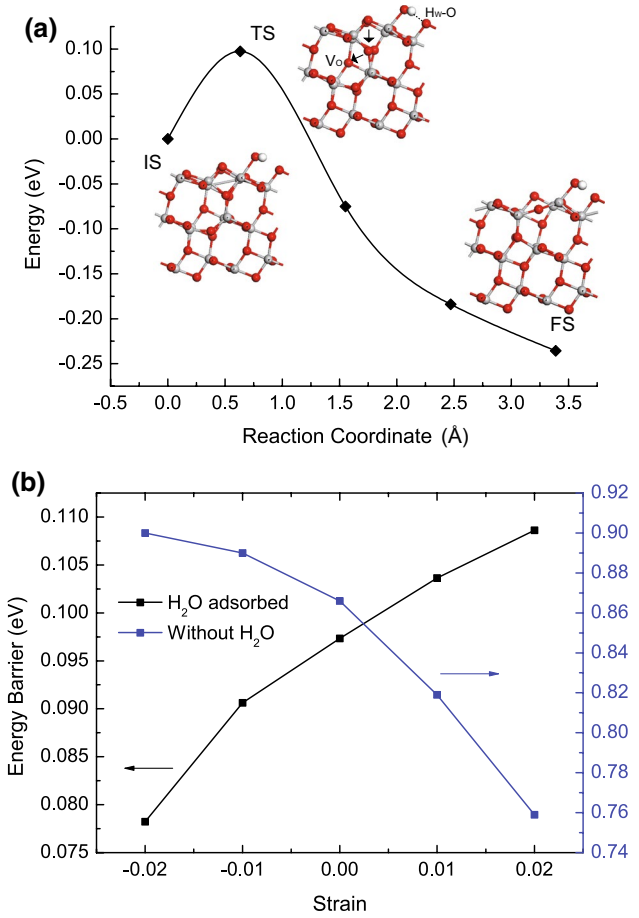

Fig. 3 **a** Diffusion of subsurface oxygen vacancy with adsorbed H_2O molecule and the corresponding energies at different images, reproduced from Ref. [30]. **b** The effect of strain on energy barrier for oxygen vacancy diffusion

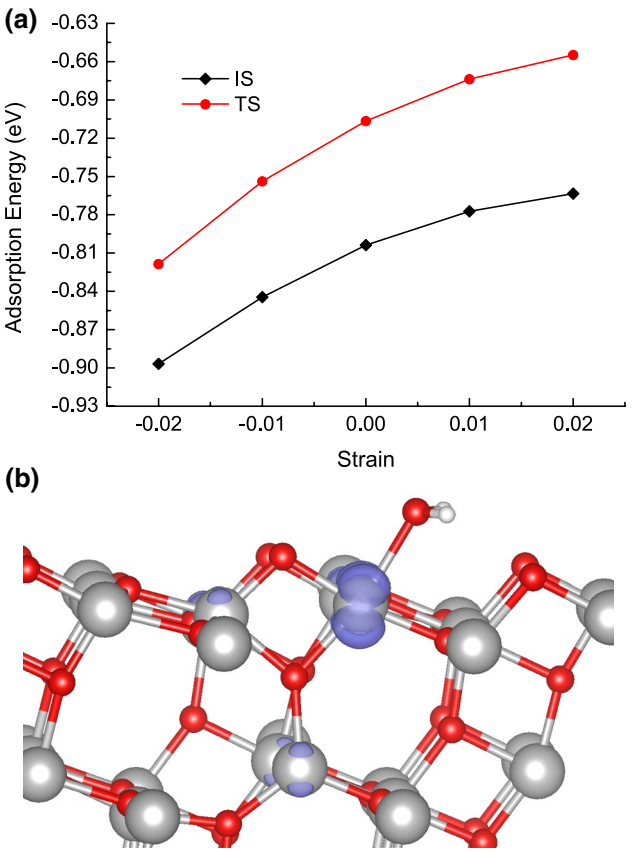

Fig. 4 The adsorption energy of water on the anatase (101) surface with varying strain. Spin localization in the triplet state for water adsorbed on the reduced surface with the isocontour value of 0.004 e/Å^3

Li and Gao [30] have comprehensively studied the interaction between water and the anatase (101) surface with a subsurface O-vacancy, indicating that water adsorption produces a relative stability of the surface O-vacancy over the subsurface one. Based on these studies, the influence of strain is explored for oxygen vacancy diffusion from V_O site to the surface with and without adsorbed water.

First, we reproduce the O-vacancy diffusion path shown in Fig. 3a [30]. A H_2O molecule strongly binds to Ti_{5c} site, of which the two H atoms form weak hydrogen bonds to bridging O atoms of the TiO_2(101) surface [43]. In the initial state (IS), O-vacancy is located at V_O site and transfers toward the surface, accompanying with the bond breaking of Ti_{5c} atom and O_{3c} atom in the transition state (TS), and subsequently, O_{3c} atom fills the defect V_O, and O_{2c} atom migrates toward the vacancy site left by O_{3c} in the final state (FS). For this path, it requires to overcome an energy barrier of 0.1 eV in accordance with that reported in Ref. [30]. On the other hand, a much larger energy of 0.87 eV is needed to drive the O-vacancy V_O to the surface with respect to the case without water adsorption on the (101) surface, which is consistent with the previous reported calculation [41].

The strain-dependent diffusion barriers are summarized in Fig. 3b. Interestingly, the results exhibit two opposite trends. For O-vacancy diffusion without water adsorbed, the energy barrier is reduced with increasing biaxial strain. It is not surprising, because intuition would suggest that an expansion of lattice weakens the interaction of atoms and therefore increases the possibility of diffusion inside the lattice. In the transition state, it features Ti_{5c}–O_{3c} bond breaking, which is closely associated with energy barrier. As a result, breaking the Ti_{5c}–O_{3c} bond becomes easier for a stretched structure, leading to a lower energy barrier. However, when H_2O molecule binds on the TiO_2(101) surface, the interplay between water and O-vacancy plays a key role in O-vacancy diffusion and water dissociation [30]. As studied here, the effect of strain on O-vacancy diffusion reverses for the (101) surface in the presence of water compared to that without water adsorption, indicating that energy barrier significantly rises with increasing strain.

To understand this result, it is worth noting that, apart from the O-vacancy diffusion, H_2O molecule largely migrates toward the neighboring bridging O_{2c} atoms on the right of Fig. 3a, confirmed by the shortened H_W–O_{2c} bond distance from 2.01 to 1.86 Å. Thus, the water adsorption energy E_a should depend on the images along the diffusion path, which can be expressed as

$$E_a = E_{c-w} - E_c + E_w \quad (2)$$

where E_{c-w}, E_c, and E_w are the total energies of water adsorbed anatase TiO_2(101) surface, clean surface, and an isolated H_2O molecule, respectively. Figure 4 shows the water adsorption energy for the initial state (IS) and transition state (TS), implying that water adsorption is facilitated by compressive strain but impeded by tensile strain. With respect to IS, the binding energy is equal to 0.8 eV, which is larger than 0.73 eV of perfect (101) surface without O-vacancies [43], attributed to the strong interplay between water and the surface O-vacancy. However, as surface strain increases, the distance of water and O-vacancy notably increases. Thus, the interaction between H_2O molecule and O-vacancy can be weakened, resulting in a lower binding energy. Similarly, the absolute value of adsorption energy for TS is reduced when the surface undergoes tensile strain. However, the reduction in binding energy for TS is slightly larger compared with that of IS, thereby producing a higher relative energy between the two states, namely producing a higher energy barrier with increasing strain.

By the above analysis, strain-induced alterations of energy barrier can be rationalized by combining the O-vacancy diffusion with water adsorption, and it is shown that strain can affect the strong interaction of H_2O molecule and the subsurface O-vacancy. To further expound the mechanism, Fig. 4b gives the spin distribution of water adsorbed TiO_2 (101) surface with the subsurface vacancy Vo. The excess electrons, originating from the O-vacancy, tend to localize on the six Ti atoms nearby, especially the under-coordinated Ti_{5c} atom binding to water, which is quietly different from the fully delocalized electrons for the defective TiO_2 without water using GGA-PBE [28, 44]. Thus, the strong interplay between water and the O-vacancy reflects in Ti_{5c} atom with localized electrons due to the presence of O-vacancy. If the surface experiences 2 % tensile strain, the bond length of Ti_{5c}–O_w (O_w from H_2O molecule) increases by 1.15 %, which weakens the interaction of water and the excess electrons, leading to the reduction in the water binding energy as shown in Fig. 4a.

4 Conclusion

In summary, we investigate the effects of strain on the band gap and oxygen vacancy diffusion for the anatase TiO_2 (101) surface by using first-principles calculations. It is found that the biaxial strain can effectively modify the band gap of the surface; for example, tensile strain reduces the band gap, which is consistent with the experiments. With respect to oxygen vacancy diffusion, energy barrier has a dependence on strain. As strain increases, it facilitates O-vacancy diffusion for the clean surface but hinders this migration for the reduced surface in the presence of water, which can be elucidated by the interplay between O-vacancy and water associated with the adsorption energy of water on the (101) surface. Nevertheless, energy barrier for the surface with water adsorption is remarkably lower compared to the clean surface. The results studied here provide the fundamental understanding for the effects of strain on surface properties of anatase (101) surface, in particular, when strain becomes significant due to surface relaxation or external forces under the nanoscale.

Acknowledgments This work is supported by AFOSR (FA9550-12-1-0159). We also acknowledge support from DARPA (W91CRB-11-C-0112).

References

1. Wang D et al (2009) ACS Nano 3:907–914
2. Han F et al (2009) Appl Catal A 359:25–40
3. Fujishima A (1972) Nature 238:37–38
4. Daghrir R, Drogui P, Robert D (2013) Ind Eng Chem Res 52:3581–3599
5. Chen X, Mao SS (2007) Chem Rev 107:2891–2959
6. Zhang Y et al (2010) ACS Nano 4:7303–7314
7. Xiang Q, Yu J, Jaroniec M (2012) J Am Chem Soc 134:6575–6578
8. Henderson MA (2002) Surf Sci Rep 46:1–308
9. Yang HG et al (2008) Nature 453:638–641
10. Yu J et al (2014) J Am Chem Soc 136:8839–8842
11. De Angelis F et al (2014) Chem Rev 114:9708–9753
12. Lazzeri M, Vittadini A, Selloni A (2001) Phys Rev B 63:155409
13. Sanches F et al (2014) Phys Rev B 89:245309
14. Selçuk S, Selloni A (2014) J Chem Phys 141:084705
15. Chen J et al (2013) J Am Chem Soc 135:18774–18777
16. Portillo-Vélez N et al (2013) Surf Sci 616:115–119
17. Labat F, Baranek P, Adamo C (2008) J Chem Theory Comput 4:341–352
18. Vittadini A et al (1998) Phys Rev Lett 81:2954
19. Sorescu DC et al (2011) J Chem Phys 134:104707
20. Lozovoi A et al (2014) J Chem Phys 141:044504
21. Liu L et al (2013) ChemPhysChem 14:996–1002
22. Linh NH et al (2015) Surf Sci 633:38–45
23. Zhang X et al (2014) Sci Rep 4:4762
24. Vittadini A, Selloni A (2002) J Chem Phys 117:353–361
25. Darkins R et al (2014) Phys Chem Chem Phys 16:9441–9447
26. Thulin L, Guerra J (2008) Phys Rev B 77:195112
27. Yin W-J et al (2010) Appl Phys Lett 96:221901
28. Aschauer U et al (2009) J Phys Chem C 114:1278–1284
29. Setvín M et al (2013) Science 341:988–991
30. Li Y, Gao Y (2014) Phys Rev Lett 112:206101
31. Blöchl PE (1994) Phys Rev B 50:17953
32. Perdew JP, Burke K, Ernzerhof M (1996) Phys Rev Lett 77:3865

33. Henkelman G, Uberuaga BP, Jónsson H (2000) J Chem Phys 113:9901–9904
34. Giannozzi P et al (2009) J Phys Condens Matter 21:395502
35. Landmann M, Rauls E, Schmidt W (2012) J Phys Condens Matter 24:195503
36. Martsinovich N, Jones DR, Troisi A (2010) J Phys Chem C 114:22659–22670
37. Sasaki T (2002) J Phys Condens Matter 14:10557
38. Shibata T, Irie H, Hashimoto K (2003) J Phys Chem B 107:10696–10698
39. Shu D-J et al (2008) Phys Rev Lett 101:116102
40. Simpson J et al (2004) Phys Rev B 69:193205
41. Cheng H, Selloni A (2009) Phys Rev B 79:092101
42. Setvin M et al (2014) Phys Rev Lett 113:086402
43. He Y et al (2009) Nat Mater 8:585–589
44. Finazzi E et al (2008) J Chem Phys 129:220–228